RSC Applied Interfaces

Accepted Manuscript

This article can be cited before page numbers have been issued, to do this please use: J. D. J. Culpepper, A. G. Frutos, J. B. Yehl, T. Chang and J. Lahiri, *RSC Appl. Interfaces*, 2025, DOI: 10.1039/D4LF00235K.

ROYAL SOCIETY OF CHEMISTRY

rsc.li/RSCApplInter

View Article Online
DOI: 10.1039/D4LF00235K

Colorless Copper-Containing Coatings With High Antimicrobial Efficacy and Formulation Versatility

Johnathan D. Culpepper[1], Anthony G. Frutos[1], Jenna B. Yehl[1], Theresa Chang[1], Joydeep Lahiri[1]*

[1]Corning Incorporated, 1 Riverfront Plaza, Corning, NY 14831, USA

* Corresponding author

Abstract

This work reports an antimicrobial (AM) copper(I)-containing additive for water-base formulations with high efficacy and minimal impact to the formulation's natural color. Determination of whether Cu^{1+} ions can be maintained for long durations of time and induce high bioactivity when used in complex aqueous environments are known technical challenges towards using copper as an antimicrobial additive. Cu^{1+} ions are the preferred oxidation state to achieve broad-spectrum AM efficacy. Also, Cu^{1+} if stabilized in a formulation, can impart low color changes relative to the Cu^{2+} ions. To this end, we developed a UV-vis spectroscopy approach to track copper speciation. We used multinuclear NMR spectroscopy on copper-based additive mixtures to also demonstrate that Cu^{1+} ions within the additive converts selected water-based formulations into antimicrobial white and clear coatings. The copper additive mixtures were made by extracting Cu^{1+} ions from a previously reported copper-glass ceramic (CGC) powder that offered high antimicrobial efficacy, but CGC powders when used directly led to unacceptably high color in white paints and clear coatings. Ligands such as phosphites were shown to promote extraction and stabilization of Cu^{1+} ions through coordination. The antimicrobial performance of the additives was tested in commercial formulations that included a white latex paint and clear coatings for wood and glass substrates. A reduction in *Staphylococcus aureus* (staph) bacteria of > 99.9% (>log 3 kill), under test conditions that simulate realistic microbial contamination, was observed for these coatings with negligible change to the original color of the coating. Here, our findings demonstrate novel advancements in the field of inorganic antimicrobial clear coatings for a range of surfaces such as in daycare, hospitality, healthcare interior spaces, automotive interiors, and consumer electronics.

View Article Online
DOI: 10.1039/D4LF00235K

Introduction

The development of new copper(I)-containing additives with high antimicrobial efficacy is strongly motivated by the fact that copper has broad-spectrum antimicrobial efficacy, copper is more abundant on earth compared to silver [1], and there are growing public health challenges concerning bioburden and transmission of harmful pathogens and observed antimicrobial resistance in high-touch surfaces [2]. In addition, there are only few examples of long-lasting commercialized Cu^{1+} antimicrobial options for white and clear coatings, which currently dominate the color space within the coatings industry.

We have previously described an antimicrobial (AM) additive for paints based on a copper glass ceramic (CGC) that kills 99.9% of bacteria and viruses in 2 hours.[3] The glass ceramic, air jet-milled into a powder with a D_{50} of ~3.5 μm, contains cuprite nanocrystals in a water-labile droplet phase interspersed in a more traditional silicate glass matrix. AM efficacy of paint films incorporating the CGC powder was demonstrated against gram positive bacteria (*Staphylococcus aureus*), gram negative bacteria (*Pseudomonas aeruginosa, Klebsiella aerogenes, and Escherichia coli*), and a non-enveloped virus (murine norovirus). The antimicrobial tests conducted used the "United States Environmental Protection Agency (EPA)" test method, which better mimic realistic microbial contamination than the classical "wet test" methods, such as JISZ2801. Unlike copper, silver-containing surfaces show high AM potency only when using the wet test, and negligible potency when using the EPA test method.

Bacteria and viruses can be classified on a scale based on their susceptibility to disinfectants; the easiest to kill are enveloped viruses (e.g. SARS-CoV-2). The hardest to kill are non-enveloped viruses, and bacterial susceptibility is in-between.[4-6] Our results against the norovirus and bacteria suggested that the paint coatings would be effective against SARS-CoV-2, the virus that causes COVID-19.[6] This hypothesis proved correct – paint coatings containing the CGC additive demonstrated 99.9% kill of SARS-CoV-2 in 2 hours. Two leading paint companies incorporated the CGC powder additive into paint products and verified effectiveness against SARS-CoV-2 and other pathogens in third party laboratories, which led to the first commercial examples of EPA-registered coatings with long-term potency against viruses, including SARS-CoV-2.

The high AM efficacy of copper is presumed to derive from interactions with germs through multiple mechanisms that include damage to the cell membrane, the generation of hydroxyl radicals through Fenton chemistry, and damage to RNA and DNA, including plasmid DNA.[7] As a result, copper is effective against all the ESKAPE pathogens and antibiotic resistant "superbugs".[8, 9] Metallic copper and copper alloy surfaces in hospitals have been shown to reduce bioburden by ~80% and decrease the spread of infection.[10-12] We have conducted a 9-month limited field study measuring bioburden surfaces such as a preschool restroom wall, and a hospital lockers painted with one of the EPA-registered antimicrobial paints and observed a significant ~60% reduction relative to the environmental controls within the same spaces.[13]

Our overarching research interest was to design a copper-based additive that maintained the AM potency of metallic copper without the same look and feel.[14] Despite the CGC powder remarkable AM potency at low loadings (~1wt% CGC in paint) that enabled >1000 paint colors, the deep orange color of the

View Article Online
DOI: 10.1039/D4LF00235K

powders precludes its use in white and clear coatings (Figure 1). Therefore, we explored fundamental understanding of coloration of the CGC powders. Our expectations was to apply such learnings from the color induced by the CGC particles when used, to advance understanding towards making a novel copper antimicrobial coatings with improved color properties. Color improvements could ensure better adoption of copper utilization as an antimicrobial.

Herein we report that there are two types of copper in the copper glass ceramic (CGC) material – a "dye" component from the water labile phase from the CGC particles, and a "pigment" component from the remaining insoluble phase (Figure 1). We hypothesized that since the insoluble "pigment" phase is the primary contributor to the CGC particles orange coloration, formulations that are modified using only the accessible labile copper in the "dye" component would result in AM efficacy with improved color properties. The key research challenge was to make copper(I)-based additive for water-based formulations with improved color while maintaining the AM potency of the original CGC powders, which requires a sufficient concentration of bioactive Cu^{1+} ions. This paper shows that nitrogen and phosphorus containing molecules that weakly coordinate to copper, like amines and phosphates, can assist in copper extraction. Stronger coordinating ligands such as phosphites significantly increased the extraction of Cu^{1+} ions from the CGC powders, while preventing their oxidation to Cu^{2+} ions in an aqueous environment. Importantly, extracts with this soluble Cu^{1+}, when added to coating formulations, showed high AM efficacy and > 5-fold lower color relative to the powdered CGC. This significant improvement in color properties enables essentially white and clear coatings, which dominate the color space of coatings for high-touch/bioburden surfaces.

Experimental Section

Materials

All reagents were purchased and used without further purification. Benzene-d^6 (C_6D_6) (>99.99%), dibenzyl phosphate (DBzP, 99%), dibutyl phosphate (DBuP, ≥97.0%), triethyl phosphite (TEP, ≥ 97.0%), trimethyl phosphite (TMP, ≥ 99.0%), and copper(II) sulfate (≥ 99.99%) were purchased from Sigma-Aldrich. Tri-n-butyl phosphite (TbuP, 94.0%) was from Alfa Aesar. 2-Amino-2-methyl-1-propanol (AMP-95) was purchased from Angus Chemical. Ethylenediaminetetraacetic acid tetrasodium salt dihydrate powder (BioReagent, suitable for cell culture, 98.5-102.0%) and 2-ethylhexyl phosphate (mixture of esters) (2-EHP) were from Millipore-Sigma. Microcrystalline diphenyl phosphate (DPP, 97%) and hydrogen peroxide (30%) were purchased from Thermo Scientific. Ethanol, and sodium hydroxide (50% w/w) were from Fisher.

Commercially available paints/coatings were selected as representative white latex paint for interior use, and clear coats for wood and glass surfaces. The latex paint was Behr Premium Plus® Ultra Eggshell Enamel Pure White 2050. The clear wood coatings were Behr Premium® Fast Drying Water-Based Polyurethane Matte B8106, and Durable Crystal Clear Varathane® Triple Thick Polyurethane Clear Satin. For glass substrates, Ferro Clear Fast Dry Urethane Water-Based Glass Coating 221 Series was used.

CGC powder was prepared as previously reported with a PSD D_{50} value of ~3.5 µm.[3] CGC powder was stored at room temperature, in air, prior to conducting all extraction experiments.

View Article Online
DOI: 10.1039/D4LF00235K

General Considerations

Paint samples were prepared by slowly adding the copper-glass ceramic (CGC) powder or CGC powder extract solution to paint with stirring by an overhead mixer. Coatings were prepared via a drawdown process on 8.7" x 5.9" Leneta White Scrub Test Panels (P123-10N) using a 7-mil stainless steel bar. A recommended wet film thickness by the manufacturer is 6.4-mil. Therefore, a 7-mil stainless bar was used to ensure a uniform dry film thickness that provides adequate coverage and protection in the absence of film cracking or peeling. Films were cured in air for at least 2 days before initial color measurements were collected, and 7 days before initial AM testing was performed. All color measurements on dried films were made using an X-Rite VS450 non-contact spectrophotometer (45/0 geometry).[15] The X-Rite spectroscopic measurements enables the quantification of film color change relative to the base coating as color controls. This was done by collecting initial color impact of a given copper additive extract recipe in the coating and monitoring whether the color stabilizes or changes in time. Color swatches used in the figures were generated by converting the measured CIE L*a*b* values to the corresponding RGB color values using a color conversion algorithm (www.convertingcolors.com).

Coatings on glass used 2" x 2" Corning® EAGLE XG® glass coupons that were cleaned with a Nordson March plasma cleaner. Glass film deposition was done via spin coating using a Specialty Coating Systems G3P-12 Spin Coater. Glass film measurements of the sample surface topography were carried out using a Zygo NewView™ 9000 3D optical surface profiler.[16]

Antimicrobial (AM) efficacy tests on duplicate 1" x 1" coupons for all substrates – i.e., Leneta panels and glass coupon using *Staphylococcus aureus* (staph) bacteria were conducted using a previously reported modified version of the United States Environmental Protection Agency (EPA) registered "dry" protocol.[17]

Extraction Procedures

Extractions were performed in a fume hood, in air, with high-purity (18 MΩ cm^{-1}) water that was not degassed. Suspensions of CGC powder (0.2g – 60g) were prepared in water (3mL – 40mL) in glass vials or centrifuge tubes. One to three equivalents of additive/ligand with respect to moles of accessible copper were added. In some experiments, an inorganic or organic neutralizer was added next. The suspensions were mixed either by sonication, or by a roller mixer for two hours, and then filtered or centrifuged to isolate the extract solution from the CGC powder. Filtration utilized a 5 mL Fisherbrand™ sterile syringe fitted with a Whatman™ Puradisc™ 25mm 0.2um PES filter. For extracts less than 15mL, centrifugation was performed using an Eppendorf 5810R centrifuge (5000 rpm, 10 mins); for extracts of 50mL, centrifugation was done using an Allegra X-30R IVD centrifuge (4700 rpm, 10 mins).

After preparation, extract solutions were stored under ambient conditions.

Copper Quantification & Method Validation

View Article Online
DOI: 10.1039/D4LF00235K

A Perkin Elmer Avio 500 inductively coupled plasma optical emission spectroscopy (ICP-OES) instrument was used to measure the copper concentration. ICP is highly sensitive but cannot differentiate between the oxidation states of copper.

To further characterize the CGC powder extracts and gain more insight into the extraction process, a simple, reliable method to quantify the amounts of Cu^{1+} and Cu^{2+} ions in the extract solution was required. Initial tests were carried out using neocuproine[18], but the method was found to be incompatible with extracts containing ligands of interest (e.g. phosphite ligands). For the CGC extraction with phosphite sampling we observed crystallization within several of neocuproine prepared samples, which could severely affect the accuracy of the copper concentration values derived (Figure S1). Therefore, an alternative spectroscopic method based on the absorbance of Cu^{2+} complexes was developed. In this method, absorbance measurements were made from two aliquots of the test solution. The amount of Cu^{2+} ions was first quantified by measuring the absorbance of aliquot one (appropriately diluted) and comparing it to a calibration curve. Because complexation of Cu^{2+} with different ligands can lead to shifts in absorbance, a strongly coordinating ligand, EDTA, was added to ensure a consistent copper complex from sample to sample. Absorbance measurements from 400nm to 900nm revealed only a single, broad peak that was assigned to (Cu^{2+})-EDTA absorption at 740 nm.[19] A separate aliquot of the test solution was taken and treated with hydrogen peroxide to oxidize the Cu^{1+} ions to Cu^{2+}. The absorbance of this second aliquot was measured and represents the total copper (Cu^{2+} + Cu^{1+}) in solution. The difference between the 2 aliquot measurements represents the amount of Cu^{1+} in the solution.

A copper calibration curve was defined using dilutions of a 20 mM $CuSO_4$/20 mM EDTA stock solution. The calibration curve was linear over the concentration range tested with an R^2 value of 0.9998. No significant differences in the calibration curves from dilutions of 20 mM copper sulfate/20 mM EDTA solutions were observed in the presence or absence of hydrogen peroxide.

NMR Experiments

Solution $^{31}P\{^1H\}$ NMR spectra were obtained using a Varian UnityInova 300 MHz NMR (^1H frequency) in conjunction with a 7T superconducting magnet. The resonance frequency of ^{31}P was 121.41 MHz. The $^{31}P\{^1H\}$ NMR spectra were acquired with a delay time of 1s, a 90° pulse width, and as a composite of 176 free induction decays. The data were processed with mNova (Mestrelab Research) using 10 Hz of line broadening.

CGC powder extracts for NMR experiments were prepared by adding 2 mL of water to 543.4 mg (0.72 mmol accessible Cu) of CGC powder and mixing until the powder was saturated and flowed in the container. 124 µL (0.72 mmol) of TEP was then added to the suspension and mixed for 1 hour. The suspension was filtered to isolate the extract.

TEP samples were prepared by adding 2 mL of water or benzene-d_6 to 124 µL (3.84 mmol) of TEP and mixing for 1 hour.

Results and Discussion

View Article Online
DOI: 10.1039/D4LF00235K

1.0 CGC Powder Extracts: Antimicrobial Efficacy, Copper Concentration, and Impact on Color

The goal of this study was to demonstrate an additive that maintained the > 3 log-kill AM efficacy of CGC powder but minimized the color impact, thereby enabling clear, colorless coatings and white coatings. This outcome requires an adequate concentration of soluble Cu^{1+} ions, resistant to oxidation (or disproportionation), but bioavailable to kill germs.

We conceptualized a process for copper extraction from CGC powder to isolate bioactive Cu^{1+} complexes in aqueous solutions. Unlike other reported aqueous copper extractions, such as from copper ores, in this study we deliberately avoided use of temperature and pressure as process levers [20, 21] to minimize the potential for copper oxidation. CGC Extracts were assessed and compared to direct use of CGC powder by incorporating them into a white latex paint and measuring paint film color and antibacterial efficacy against *Staphylococcus aureus*. In the first series of experiments, the following extract process levers were assessed: solvent, pH, and copper-coordinating ligands.

1.1 Solvent and pH Impact on CGC Powder Extraction

Given the trend toward water-based formulations, the extraction of copper from CGC powders using either water or ethanol was evaluated. CGC powder extraction using only water or ethanol, with or without sonication, did not lead to latex paint films with any substantial AM efficacy (~0.6 log kill). Doubling the volume of CGC powder extract added to the paint did not significantly improve AM efficacy (0.7-1.0 log kill, see Table 1). These findings suggested that CGC powder extracts from water or ethanol contained negligible amounts of copper. ICP-MS measurements confirmed that only ~13ppm of copper was present in the extract solution.

Latex paint coatings incorporating CGC powder at 1wt% give reproducible and long-term AM efficacy. Our finding that water extracts of CGC powders give low AM efficacy suggest that i) CGC particle contact is required to achieve kill [22, 23]; or ii) paint formulation constituents play a role in the “in-situ” extraction of soluble copper from the CGC powders. A necessary component of latex paint formulations is an organic or inorganic Brønsted-Lowry base (“neutralizer”) that is added to adjust the pH within a range (pH 8-9) that stabilizes the emulsion. Neutralizers are also co-dispersant corrosion inhibitors for pigments in water-based coatings. CGC extract experiments with sodium hydroxide or the organic base 2-amino-2-methyl-1-propanol (AMP-95), a common neutralizer in paint manufacturing, resulted in colored copper complexes. Extract solutions with sodium hydroxide were yellow and extract solutions with AMP-95 were deep purple. Paint films incorporating these extracts showed improved AM efficacy (2.4 – 5.0 log kill, see Table 1, Exp #5-8) relative to paint films made with extracts from pure water (~ 0.6 log kill), but resulted in films with color (ΔE^* values of 4-10) that was similar to, or worse than, paints films with the CGC powder itself ($\Delta E^* \sim 7$). The improvement in AM efficacy was hypothesized to be due to better copper extraction via coordination of the Brønsted-Lowry bases with copper[24], and prompted the assessment of other classes of coordinating ligands.

1.2 CGC Powder Extraction with Phosphates

View Article Online
DOI: 10.1039/D4LF00235K

There is a growing body of literature on copper extractions from ores that shows the critical role of metal coordination chemistry in aqueous environments.[25, 26] We have previously demonstrated that thiocyanate ligands added to CGC powders decreased coloration, presumably due to the in-situ formation of cuprous thiocyanate, but the resulting complex had significantly lower AM activity (unpublished results). This led us to investigate weakly coordinated ligands that could enhance extraction while preserving bioavailability. We selected phosphates as a representative example of a moiety that weakly coordinates to copper (via the lone pair of electrons in the phosphate group (-P=O or -P-O^-)) and assessed the impact of this class of molecules on copper extraction, AM efficacy, and color.

Aqueous extracts from CGC powder made with either dibenzyl phosphate (DBzP) or diphenyl phosphate (DPP), in the presence or absence of AMP-95, were incorporated into paint films, and color and AM efficacy were measured (Table 1, Exp #9-14). Here we used AMP-95 within extraction mixtures as a Lewis base to understand pH effects on copper extraction from the CGC powders in the presence of phosphates. AMP-95 also served other purposes. To deprotonate the phosphate, assists with the potential for copper-phosphate molecule coordination, and AM activity. Key observations from these experiments were: 1) AM efficacy was higher for paint films made from extracts with phosphate molecules in the presence of AMP than in the absence of AMP; 2) the presence of AMP in the extract solution yielded paint films with ΔE* values 1-2 units higher relative to paint films made with extracts without AMP; 3) increasing the ratio of phosphate relative to CGC powder during the extraction gave paint films with higher AM efficacy. These data suggested that converting a phosphate to its respective salt ($RNH_3^+[Ph_2PO_4^-]$) with a (-P-O^-) bond was important to assist the CGC-phosphate extractions and subsequent AM activity, and confirmed our hypothesis that Lewis bases (like a deprotonated phosphate) and metal chelation play an important role in extraction of copper from CGC powder.[24]

A more concentrated extract is desirable when used as an additive in a formulation because it enables effective copper concentrations in the formulation without unduly diluting the formulation and impacting key properties (e.g. coalescence). When we attempted to use phosphates to make concentrated extracts from larger amounts of CGC powders (≥32wt%), we observed several processing challenges that were not manifest when conducting extractions from smaller amounts of CGC powder (<32wt%). For example, with diphenyl phosphate (DPP) we observed severe particle caking, meaning that the CGC particles were not free flowing in the extract solution and became densely packed, possibly due to the hydrophobicity of the phosphate molecule and/or an increased amount of aggregates formed.[27, 28] As a result of this caking, the extract volume yields were ~15-20% lower. We tested phosphates without a phenyl ring, including dibutyl phosphate (DBuP) and 2-ethyl hexyl phosphate (2-EHP) (see Figure 2). CGC powder extracts with 2-EHP (made with CGC powder at > 32wt% during the extraction) gelled over time (minutes to days, depending on the concentration).[24, 29, 30] DBuP gave an undesirably high background AM efficacy (~2.5 log kill) when added to paint films with no copper present. Because of the processing challenges associated with phosphates, we decided to abandon using them as viable additives for copper extraction.

1.3 CGC Powder Extraction with Phosphites

The most bioactive form of copper is Cu^{1+} and our goal with extracting CGC powders was to isolate and stabilize a high concentration of these ions.[31] Because Cu^{1+} ions are a soft Lewis acid, we investigated

View Article Online
DOI: 10.1039/D4LF00235K

soft Lewis bases as strongly coordinating bases.[32] Recently, it was shown that methoxy substituted phosphoramidite ligands, with structural features similar to a phosphite (i.e. a phosphorous(III) atom and P-O bonds), coordinate to platinum(II) and result in water-soluble platinum complexes [30]. In addition to coordinating with copper(I), phosphites can also act as antioxidants.[33, 34] Phosphites have been used as additives in coatings, for purposes other than metal complexation or redox stabilization.[35]

To determine whether strongly coordinating, soft Lewis bases such as phosphites aid in copper extraction, we first tested triethyl phosphite (TEP) in aqueous or ethanolic extracts from CGC powder. Paint films from aqueous extracts incorporating TEP gave significantly higher AM efficacy relative to ethanolic extracts incorporating TEP (4.5 log kill vs 2 log kill, see Table 1, Exp #15-19). The use of AMP-95 did not significantly improve AM efficacy, but rather resulted in films with poorer color (ΔE* ~4.4) (Table 1, Exp #17-18). Importantly, we identified an extraction condition that gave high AM activity and significantly improved color (5.13 log kill and ΔE* = 0.9). Unlike the attempts at generating concentrated extracts with phosphates, we found that conducting extractions with TEP from higher amounts of CGC powder (25, 39 and 53wt%) did not present processing challenges.

Copper speciation was measured for aqueous extracts with TEP from varying amounts of CGC powder using the UV-vis method described earlier (see materials and methods). The correlation between this UV-vis method and ICP-OES for total copper was excellent (R^2 value of 0.995) and demonstrated the reliability of the UV-vis method (Figure 3A). High levels of total copper were measured (7,620ppm, 12,320ppm, and 18,120ppm for the 25wt%, 39wt%, and 53wt% extractions, respectively) with Cu^{1+}/Cu_{total} ratios > 80%. Extract solutions were stored in glass bottles in air at room temperature. Under these storage conditions the Cu^{1+}/Cu_{total} ratio stayed high and relatively constant for months (Figure 3B).

A homologous series of phosphites (methoxy, ethoxy, butoxy substituted) was briefly tested in CGC powder extractions to assess how substituents on the phosphorus impact extraction of copper. Quantification of copper concentration in different CGC powder extracts by UV-vis showed the following trend: trimethyl phosphite (TMP) > triethyl phosphite (TEP) > tributyl phosphite (TBuP). Most importantly, of the three phosphite CGC powder extractions, TEP gave the highest Cu^{1+}/Cu_{Tot} ratio (86%).

1.4 Interaction of Copper and Phosphites

Having demonstrated that use of TEP in the CGC powder extraction process yields extract solutions with high concentrations of stable Cu^{1+}, we desired to understand whether there is a direct interaction between the phosphite and Cu^{1+}.

$^{31}P\{^{1}H\}$ NMR spectra were collected to elucidate TEP reactivity in water and with Cu^{1+} from CGC powder (see Figure 4). TEP in deuterated benzene-d^6 gave a sharp signal at 135 ppm which agrees with literature assignment of the compound.[36] As expected, the phosphorus signal of the TEP in water showed evidence of hydrolysis with the signal shifting substantially up field to ~8ppm, which is within the expected range for formation of diethyl phosphonate.[37] The NMR spectrum of an aqueous extract of CGC powder with TEP shows a broad, asymmetrical quartet centered at 118 ppm that was not present in the spectrum of TEP alone (either in benzene-d^6 or water). We believe that this NMR signature is indicative of copper(I)-

View Article Online
DOI: 10.1039/D4LF00235K

phosphite complexation. Tisato and Refosco synthesized water-soluble copper(I) phosphine complexes and the ^{31}P CPMAS spectrum of the material showed similar features of phosphorous-copper coupling.[38] The quartet feature arises from spin-spin coupling of the phosphorus nuclei to the copper nuclei (^{63}Cu and ^{65}Cu, I=3/2). For phosphine P-C bonds, one would expect the phosphine copper(I) complex to have a down-field chemical shift relative to the free phosphine. For a phosphite P-O copper(I) complex, an up-field chemical shift relative to the free phosphite is expected [39], in alignment with the observed up-field shift of the quartet centered at 118 ppm.

We tested if performing the extraction with TEP at a higher concentration of CGC powder (53wt%), and longer time for extraction (48 hours before isolation of the extract) resulted in any variances from the NMR spectrum observed with a lower concentration of CGC powder. The data showed that the phosphorus copper coupling and additional phosphorus features were present regardless of the concentration of CGC powder during the extraction.

To determine the copper phosphorus coordination environment, we applied an approach reported by Bowmaker et al.[40] and Muetterties et al.[41] who demonstrated that the scalar coupling constant for the ^{31}P-metal bond depends only on the number of phosphorus(III) ligands coordinated to the metal(I) center. When this approach is applied to the CGC-phosphite complex, the $^{1}J_{Cu\text{-}P}$ value is 1.24 kHz, indicating that a 2-coordinated phosphito copper(I) complex was formed.[29, 38, 40-44]

Other classes of ligands beyond those described in this work (e.g. sulfur-based ligands) could be similarly engineered to bind and stabilize Cu^{1+} ions, but not too tightly to ensure bioavailability.

2.0 CGC Powder Extract Performance in Multiple Coatings

The primary objective for this study was to prepare a copper antimicrobial additive with improved color performance relative to CGC powder that would enable true whites and clear, colorless coatings. In the following discussion, we outline the learnings from incorporating CGC powder extracts into a latex paint, two different polyurethane clear wood coatings, and a transparent glass coating. These examples were chosen to highlight the improvement in the potential color palette for previously demonstrated paint coatings and to show applicability to previously inaccessible clear coatings for high-touch products, spanning furniture to consumer electronics.

Paint colors are obtained by mixing in pure colorants, or combinations thereof to a base paint. The lightest pastel shades are obtained by adding very small amounts of colorant to a base containing high amounts of a white pigment (titanium dioxide). If the base paint itself has coloration due to the copper, the color space for the lighter shades becomes fundamentally inaccessible. Therefore, our experiments were aimed at studying AM efficacy and improvement in color due to the CGC powder extract relative to the CGC powder. We assessed the AM efficacy of white latex paint films made with Behr 2050 paint that incorporated CGC powder extracts. As shown in Figure 5A, different additives used for CGC powder extraction influence the AM efficacy of the dry paint film. In the absence of a CGC powder extract, the background AM efficacy of the paint film is low. Extracts with the phosphate DPP showed > 3 log kill in the presence or absence of the organic base AMP-95, with higher kill observed in the absence of AMP-95.

View Article Online
DOI: 10.1039/D4LF00235K

Extracts with the phosphite TEP showed > 5 log kill, similar to films with CGC powder. All films with CGC powder extracts showed lower color shift relative to films with CGC powder (Figure 5B). Most interestingly, the CGC-TEP extract gave films with the lowest color shift (ΔE* value ~ 0.9), a reduction of 6.5 units compared to the CGC powder, which represents an ~8 fold improvement. The visual representation of the paint samples in Figure 5C shows only a subtle color difference that is barely distinguishable to the untrained eye between the control paint and the paint containing the CGC-TEP extract.

Two water-based polyurethane wood coatings were tested to assess performance of CGC powder extracts and CGC powder in clear, colorless formulations. CGC powder extracts or CGC powder were incorporated into polyurethane films with different sheens (Behr matte polyurethane and a Varathane satin polyurethane). As shown in Figure 6A, the controls with no copper exhibited low AM efficacy. Increased loading of the CGC powder (5wt%) and CGC-TEP extract (1000ppm copper) was required to achieve high AM efficacy in both formulations; these loadings are substantially higher than those required in the Behr 2050 latex paint to achieve similar AM efficacy. We also observed that the AM efficacy was higher in the Varathane formulation relative to the Behr formulation, likely due to differences in the constituents of the different formulations. CGC powder and CGC-TEP extracts both gave films with high AM efficacy but the color performance of films with the extracts was far superior (Figure 6B). Specifically, relative to films with CGC powder, films of the Behr formulation incorporating CGC-TEP extracts had a 4.3x (46 units) lower ΔE* value, while films of the Varathane formulation had a 14.6x (64 units) smaller ΔE*. The visual improvements in color are striking (Figure 6C).

CGC powder extracts prepared with a different phosphite tributyl phosphite (TBuP), were made and incorporated into films of the latex paint and the two wood coatings. AM efficacy for all films was low (< 2 log kill). Copper speciation by UV-vis showed that no copper(I) was present.

A Ferro 221 Series coating was used to demonstrate CGC powder extracts for clear, colorless coatings on glass. Films of this formulation on glass were prepared via spin coating. To lower the risk of copper(I) oxidation during curing, we tested flash curing of the samples at several temperatures (25°C - 120°C). Although the highest AM efficacy was observed for films cured at 25°C, all three cure conditions gave > 3 log-kill efficacy (Figure 7A). Optical transmission was measured for each coating and showed > 89% transmission in the wavelength range of 350 - 750nm. The absorbance values are within ~2 percentage points of bare glass controls (Figure 7B). Finally, we collected Zygo surface profilometry measurements and observed that thickness and surface roughness were similar for control films and films with the CGC powder extracts (see supplementary information).

Conclusions

There is significant societal value to inherently antimicrobial surfaces. Episodic cleaning with wipes and disinfectants is fundamentally error prone, and impractical for daily implementation outside of specialized settings such as surgical environments due to the diligence required.[6] Materials for antimicrobial surfaces span inorganics (e.g. Cu, Ag, Zn) and organics (e.g. quaternary ammonium compounds). Among these, copper-containing surfaces are unique due to their ability to kill germs under test conditions that simulate realistic microbial contamination and in their broad spectrum of efficacy against bacteria (gram

View Article Online
DOI: 10.1039/D4LF00235K

positive and gram negative) and viruses (enveloped and non-enveloped). The major challenges with copper-based antimicrobials are coloration and their propensity to oxidize. This work reports a novel copper(I)-based additive that enables high-efficacy antimicrobial water-based formulations with minimal impact to the native color, potentiating white and clear coatings. Ligands such as phosphites offer a route to additives with high concentrations of copper(I) ions resistant to oxidation, which is required for shelf life and long-term efficacy. These results could enable high-touch clear coatings across a range of applications such as daycare, hospitality and healthcare interior spaces, automotive interiors, and consumer electronics. There are significant commercial and regulatory challenges that must be overcome for broad deployment of antimicrobial surfaces, but the first step is the technical demonstration of approaches that offer high antimicrobial efficacy without compromising the aesthetics of the target surface application. Moreover, we demonstrated that the copper(I)-containing additive can be incorporated into water-based formulations with very low color impact and > 99.9% (>log 3 kill) against *Staphylococcus aureus* (staph) bacteria under realistic microbial contamination test conditions which may enable promising opportunities for future research materials design, and development that may eventually facilitate large-scale deployment of colorless copper antimicrobial coatings.

Author contributions

Conceptualization: Johnathan D. Culpepper, Anthony G. Frutos, Theresa Chang, Joydeep Lahiri
Formal analysis: Johnathan D. Culpepper, Anthony G. Frutos
Investigation: Johnathan D. Culpepper, Jenna B. Yehl
Methodology: Johnathan D. Culpepper, Anthony G. Frutos
Project administration: Anthony G. Frutos
Writing – original draft: Johnathan D. Culpepper, Joydeep Lahiri
Writing – review & editing: Johnathan D. Culpepper, Anthony G. Frutos, Joydeep Lahiri

Conflicts of interest

Corning sells the copper-glass ceramic powder antimicrobial additive (Corning ® Guardiant®) described in this manuscript.

Acknowledgements

Ashley R. Clark – Color measurements
Jackie L. Kurzejewski – Antimicrobial efficacy measurements
David L. Baker – Zygo measurements
Eric Null & Blake E. Johnson – Support for UV-vis measurements
Brian Rice – ICP measurements

Notes and References

1. Grochala, W. and Z. Mazej, *Chemistry of silver (II): a cornucopia of peculiarities.* Philosophical Transactions of the Royal Society A: Mathematical, Physical and Engineering Sciences, 2015. **373**(2037): p. 20140179.
2. Mäki, A., et al., *Microbiota shaping and bioburden monitoring of indoor antimicrobial surfaces.* Frontiers in Built Environment, 2023. **9**: p. 1063804.

View Article Online
DOI: 10.1039/D4LF00235K

3. Gross, T.M., et al., *Copper-containing glass ceramic with high antimicrobial efficacy.* Nature communications, 2019. **10**(1): p. 1-8.
4. Russell, A., *Bacterial resistance to disinfectants: present knowledge and future problems.* Journal of Hospital infection, 1999. **43**: p. S57-S68.
5. Maillard, J.-Y. and M. Pascoe, *Disinfectants and antiseptics: mechanisms of action and resistance.* Nature Reviews Microbiology, 2024. **22**(1): p. 4-17.
6. Basak, S.S. and A. Adak, *Physicochemical methods for disinfection of contaminated surfaces–a way to control infectious diseases.* Journal of Environmental Health Science and Engineering, 2024: p. 1-12.
7. Cross, J., et al., *Killing of Bacillus spores by aqueous dissolved oxygen, ascorbic acid, and copper ions.* Applied and environmental microbiology, 2003. **69**(4): p. 2245-2252.
8. Xie, M., et al., *Antibacterial nanomaterials: Mechanisms, impacts on antimicrobial resistance and design principles.* Angewandte Chemie International Edition, 2023. **62**(17): p. e202217345.
9. IACONI, O.-S., et al., *The Public health problem and resistant bacteria in lowand middle-income countries.* One Health & Risk Management, 2024. **5**(1): p. 34-42.
10. Schmidt, M.G., et al., *Sustained reduction of microbial burden on common hospital surfaces through introduction of copper.* Journal of clinical microbiology, 2012. **50**(7): p. 2217-2223.
11. Salgado, C.D., et al., *Copper surfaces reduce the rate of healthcare-acquired infections in the intensive care unit.* Infection Control & Hospital Epidemiology, 2013. **34**(5): p. 479-486.
12. Michels, H.T., et al., *From laboratory research to a clinical trial: copper alloy surfaces kill bacteria and reduce hospital-acquired infections.* HERD: Health Environments Research & Design Journal, 2015. **9**(1): p. 64-79.
13. Hiras, J., et al., *Reduction of bioburden on large area surfaces through use of a supplemental residual antimicrobial paint.* Plos one, 2024. **19**(9): p. e0308306.
14. Navaratnam, S., et al., *Designing post COVID-19 buildings: Approaches for achieving healthy buildings.* Buildings, 2022. **12**(1): p. 74.
15. Feld, R., *Guidelines for Measuring Colours: Optimising Coating Processes.* IST International Surface Technology, 2013. **6**(2): p. 46-47.
16. Yi, S., et al., *Angle-based wavefront sensing enabled by the near fields of flat optics.* Nature communications, 2021. **12**(1): p. 6002.
17. Mitchell, A.L., et al., *Antimicrobial Fe2O3-CuO-P2O5 glasses.* Scientific Reports, 2023. **13**(1): p. 17472.
18. Tütem, E., R. Apak, and F. Baykut, *Spectrophotometric determination of trace amounts of copper (I) and reducing agents with neocuproine in the presence of copper (II).* Analyst, 1991. **116**(1): p. 89-94.
19. Noguchi, M., et al., *Photoinduced degradation of fluorescence and formation of copper nanoparticles in sol–gel silica doped with flavins.* Journal of non-crystalline solids, 2011. **357**(15): p. 2966-2969.
20. Godirilwe, L.L., et al., *Extraction of copper from complex carbonaceous sulfide ore by direct high-pressure leaching.* Minerals Engineering, 2021. **173**: p. 107181.
21. Velásquez-Yévenes, L. and V. Quezada-Reyes, *Influence of seawater and discard brine on the dissolution of copper ore and copper concentrate.* Hydrometallurgy, 2018. **180**: p. 88-95.
22. Mathews, S., et al., *Contact killing of bacteria on copper is suppressed if bacterial-metal contact is prevented and is induced on iron by copper ions.* Applied and environmental microbiology, 2013. **79**(8): p. 2605-2611.
23. Sunada, K., M. Minoshima, and K. Hashimoto, *Highly efficient antiviral and antibacterial activities of solid-state cuprous compounds.* Journal of hazardous materials, 2012. **235**: p. 265-270.

View Article Online
DOI: 10.1039/D4LF00235K

24. *To show that Brønsted-Lowry bases can also be ligands, in methanolic environment Nakajima et al, demonstrated a multistep reaction of Cu(NO3)23H2O with amino alcohols to form a copper precursor. Interestingly, they further demonstrated that the copper precursor reacts with deprotonated diphenyl phosphate (DPP) to form an inner-sphere coordinated [Ph2PO4-] tridentate amino alcohol complex [Cu(H2L)(PhO)2PO2](NO3), as greenish blue crystals [24].*
25. Valenzuela, F., et al., *Removal of copper ions from a waste mine water by a liquid emulsion membrane method.* Minerals Engineering, 2005. **18**(1): p. 33-40.
26. de Lemos, L.R., et al., *Copper recovery from ore by liquid–liquid extraction using aqueous two-phase system.* Journal of hazardous materials, 2012. **237**: p. 209-214.
27. Kloda, M., et al., *Phosphinic acids as building units in materials chemistry.* Coordination Chemistry Reviews, 2021. **433**: p. 213748.
28. Nakajima, T., et al., *Systematic Synthesis of Di-, Tri-, and Tetranuclear Homo-and Heterometal Complexes Using a Mononuclear Copper Synthon with a Tetradentate Amino Alcohol Ligand.* European Journal of Inorganic Chemistry, 2016. **2016**(17): p. 2764-2773.
29. Ben-Nissan, B., et al., *31P NMR studies of diethyl phosphite derived nanocrystalline hydroxyapatite.* Journal of sol-gel science and technology, 2001. **21**: p. 27-37.
30. *Gelled extracts obtained from 67wt% CGC powder had interesting properties that were not investigated further because of the scope of this study. However, we found that the copper-phosphate gel could be dissolved in excess water and maintain bioactivity after several months of storage in air, and the gel maintained a consistent color when stored in air for 11 months. Others have investigated sol-gel approaches to preparing copper oxide films for dip-coatings for various applications [41].*
31. Salah, I., I.P. Parkin, and E. Allan, *Copper as an antimicrobial agent: Recent advances.* RSC advances, 2021. **11**(30): p. 18179-18186.
32. Pearson, R.G., *Hard and soft acids and bases, HSAB, part II: Underlying theories.* Journal of Chemical Education, 1968. **45**(10): p. 643.
33. Humphris, K. and G. Scott, *Mechanisms of antioxidant action. Phosphite esters.* Pure and Applied Chemistry XIth, 1973. **36**(1-2): p. 163-176.
34. Schwetlick, K. and W.D. Habicher, *Organophosphorus antioxidants action mechanisms and new trends.* Die Angewandte Makromolekulare Chemie: Applied Macromolecular Chemistry and Physics, 1995. **232**(1): p. 239-246.
35. Husár, B., et al., *The formulator's guide to anti-oxygen inhibition additives.* Progress in Organic Coatings, 2014. **77**(11): p. 1789-1798.
36. Stothers, J. and J. Robinson, *NMR SPECTRA OF O, O-DIALKYLORGANOPHOSPHORUS ESTERS. P31CHEMICAL SHIFTS BY HETERONUCLEAR SPIN DECOUPLING.* Canadian Journal of Chemistry, 1964. **42**(4): p. 967-970.
37. Jackson, W.R., et al., *The Stereochemistry of Organometallic Compounds. XXXVIII. Regio-and Stereo-control in the Rhodium-Catalyzed Hydroformylation of Some Alkenyl Phosphites.* Australian Journal of Chemistry, 1992. **45**(5): p. 823-834.
38. Tisato, F., et al., *Synthesis, characterization, and crystal structure of the water soluble copper (I) complex with trisulfonated triphenylphosphine.* Inorganic Chemistry, 2001. **40**(6): p. 1394-1396.
39. Lee, K., et al., *Modifying phosphorus (III) substituents to activate remote ligand-centered reactivity in triaminoborane ligands.* Organometallics, 2020. **39**(13): p. 2526-2533.
40. Bowmaker, G.A., et al., *Structural, vibrational and solid-state NMR studies of the halogenocuprate (I) complexes [(PPh3) 2CuI2]-and [(PPh3) CuI3Cu (PPh3)].* Inorganic Chemistry, 1989. **28**(20): p. 3883-3888.

View Article Online
DOI: 10.1039/D4LF00235K

41. Muetterties, E. and C. Alegranti, *Solution structure and kinetic study of metal-phosphine and-phosphite complexes. I. Silver (I) system.* Journal of the American Chemical Society, 1972. **94**(18): p. 6386-6391.
42. Kroeker, S., et al., *Anisotropy in the31P, 63/65Cu Indirect Spin–Spin Coupling and31P Nuclear Shielding Tensors of Linear Copper (I) Phosphines.* Journal of Magnetic Resonance, 1998. **135**(1): p. 208-215.
43. Asaro, F., et al., *63Cu-31P coupling constants and 63Cu quadrupole couplings from 31P CP/MAS spectra of copper (I)—phosphine complexes with aryldithiocarboxylates or benzoate.* Solid State Nuclear Magnetic Resonance, 1997. **8**(2): p. 81-88.
44. King, R.W., T. Huttemann, and J. Verkade, *63 Cu–and 65 Cu–31 P spin–spin coupling in copper (I) trialkyl phosphite complexes.* Chemical Communications (London), 1965(21): p. 561a-561a.

Table 1. Experimental parameters for copper glass-ceramic (CGC) powder extractions, incorporation of extracts into paint, and results of antimicrobial and color measurements.

Exp #	CGC powder (g)	Solvent (mL)[a]	AMP-95 (µL)	Additive[b]	CGC powder (wt%)[c]	Paint (g)[d]	Extract volume (mL)	Log Kill[e]	Paint film color (ΔE*)[f]
Solvent Studies									
1	0.51	3.0*	-	-	17.7	50.4	2.5	0.59	0.7
2	0.51	3.0			14.6	50.3	2.5	0.60	0.5
3	1.0	6.0			14.3	50.0	5.0	0.73	0.6
4	1.0	6.0			14.3	50.2	5.0	1.08	0.5
pH Studies									
5	1.0	6.0	-	NaOH (200µL)	13.7	50.5	5.0	3.42	1.0
6			200	-	0.52	50.0		2.39	3.8
7			200			50.5		2.46	3.5
8	5.0	8.9	1770		0.30	50.0	8.0	4.98	9.5
Phosphate Studies									
9	1.0	6.0	-	DBzP (0.37g, 1X)	13.6	50.0	5.0	2.05	1.1
10			200		13.3			4.76	3.0
11			200	DPP (0.34g, 1X)	13.3			3.65	3.1
12								4.25	2.8
13			-	DPP (1.02g, 3X)	12.5			4.86	2.5
14			200		12.2			5.28	3.6
Phosphite Studies									
15	0.51	3.0*	-	TEP (345µl, 3X)	15.9	50.4	2.5	1.95	0.8
16	0.51	3.0	-		13.3	50.2	2.5	4.45	2.4
17	0.50	5.0	1040		7.36	50.0	5.0	4.98	4.1
18	5.0	8.9	1770		31.5	50.0	8.0	4.98	4.6
19	1.0	6.0	-	TEP (690µl, 3X)	13.1	50.0	6.0	5.13	0.9

a – solvent is water unless indicated by a * in which case it is ethanol
b – DBzP = dibenzyl phosphate; DPP = diphenyl phosphate; TEP = triethyl phosphite
c – weight % of the CGC powder in the extraction process: [Mass of CGC powder/ Σ (Mass of all extract components)] x 100
d – Behr Premium Plus® Eggshell Enamel Ultra Pure White® 2050
e – 2-hour antimicrobial "dry test" results against the bacteria *S. aureus*
f – color measurements are referenced to a paint film with no extract added

View Article Online
DOI: 10.1039/D4LF00235K

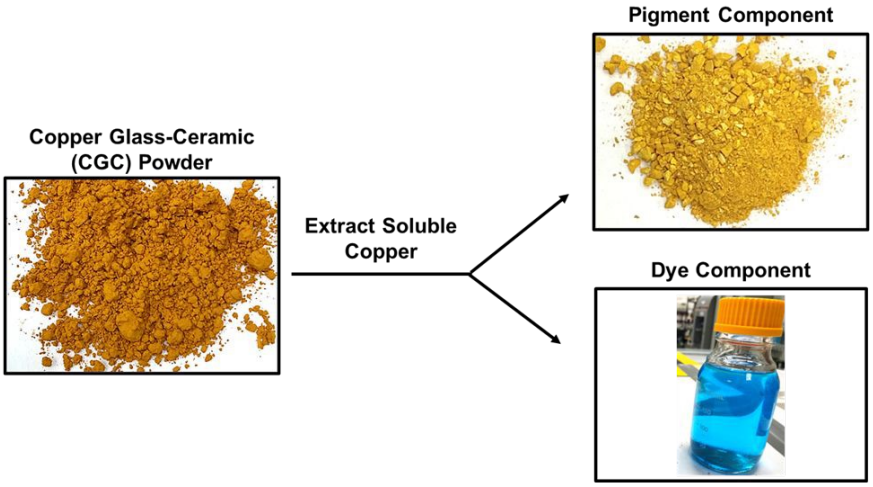

Figure 1. Copper glass-ceramic (CGC) powder has a water-soluble phase that can be extracted (dye component) and a water-insoluble phase (pigment component). The pigment component is the primary contributor to color shift and the dye component with the soluble copper species is the primary contributor to antimicrobial efficacy.

View Article Online
DOI: 10.1039/D4LF00235K

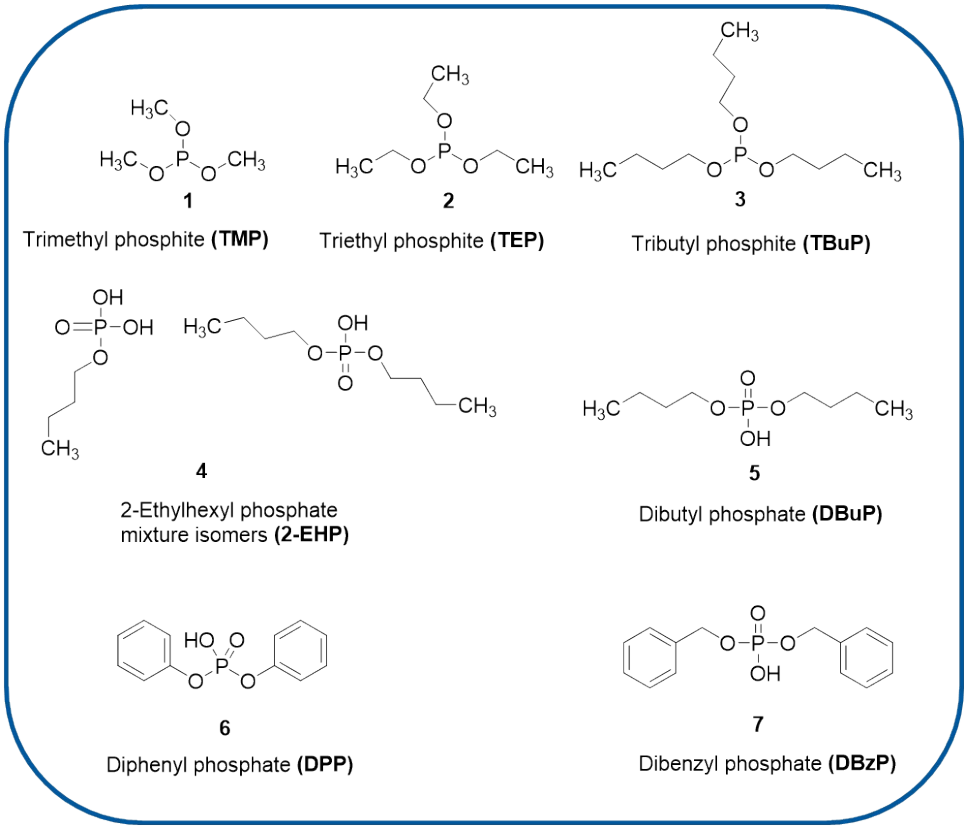

Figure 2. Molecular structures of phosphite and phosphate chemicals tested in extractions from copper glass-ceramic powder.

View Article Online
DOI: 10.1039/D4LF00235K

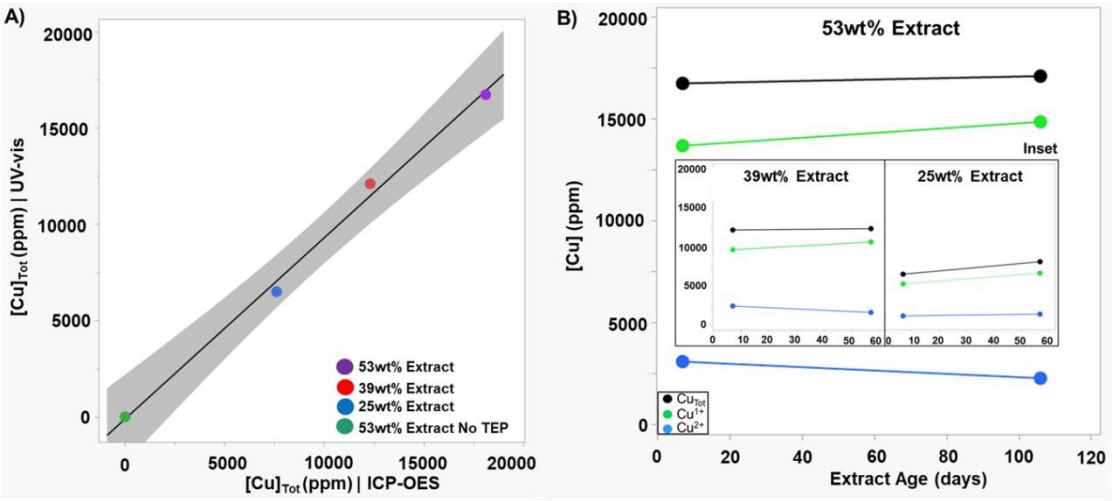

Figure 3. Measurement of copper in copper glass-ceramic (CGC) powder extracts. **A.** Scatter plot of total copper in CGC powder extracts (25, 39, 53wt% with 1 equivalent of TEP) measured by inductively coupled plasma – optical emission spectroscopy (ICP-OES) and an ultraviolet-visible (UV-vis) spectroscopy methods. The two methods are highly correlated as shown by an R^2 value of 0.995. An advantage of the UV-vis method is the ability to quantify the amount of copper ions in each oxidation state. **B.** Amount of Cu^{+1}, Cu^{+2} and total copper in 3 different CGC powder extracts measured over time by the UV-vis method.

View Article Online
DOI: 10.1039/D4LF00235K

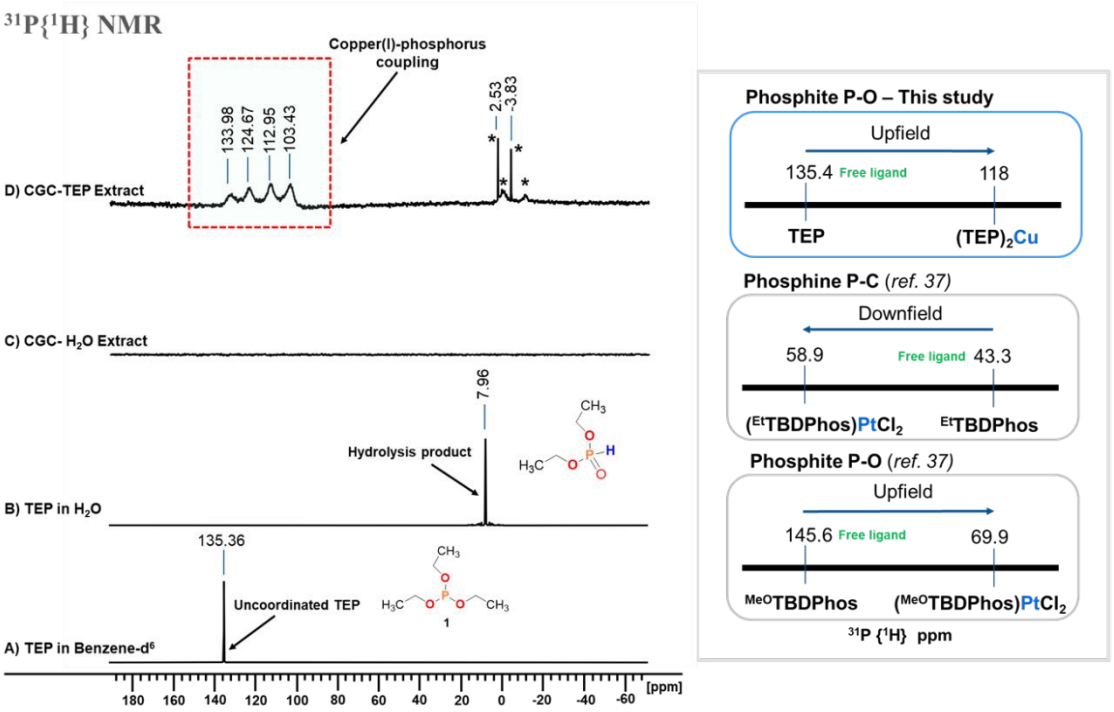

Figure 4. *Left* – $^{31}P\{^{1}H\}$ NMR spectra of copper glass-ceramic (CGC) powder extracts with triethyl phosphite (TEP) in water. **A.** Spectrum of neat TEP in deuterated benzene. **B.** Within 1 hour, TEP in water alone hydrolyzes to diethyl phosphonate. **C.** CGC powder extracts with water alone shows no phosphorous signal. **D.** CGC powder extracts with TEP show a quartet centered at 118 ppm associated with Cu(I)-phosphorus coupling. The peaks with asterisks are unassigned. *Right* – An upfield chemical shift observed in this study is consistent with a phosphite organophosphorous(III) ligand coordinated to a transition metal [37].

View Article Online
DOI: 10.1039/D4LF00235K

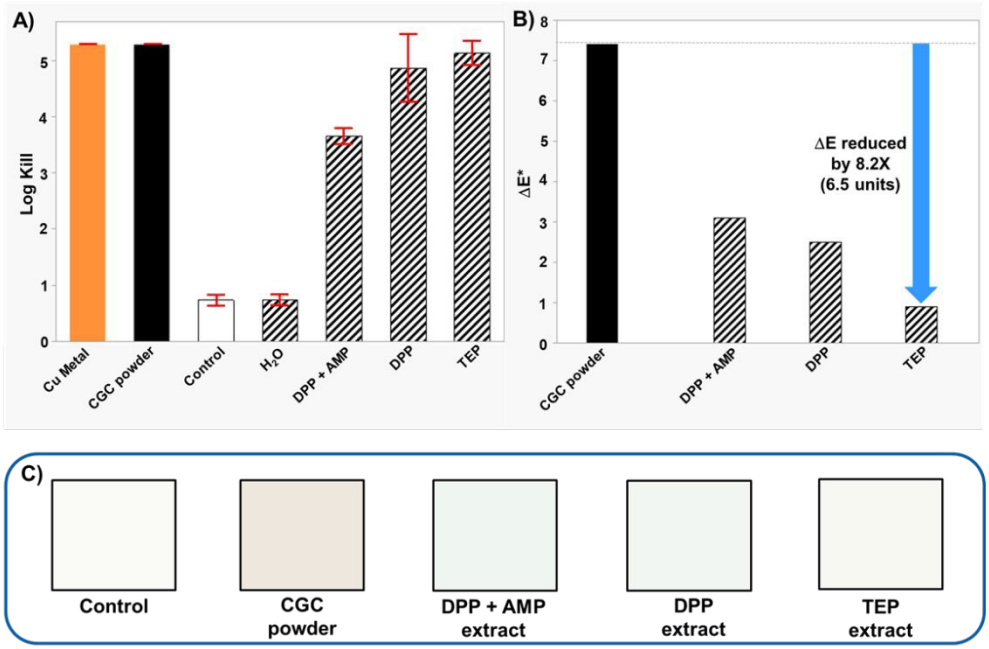

Figure 5. Antimicrobial efficacy and color results for Behr 2050 latex paint dry films incorporating copper glass-ceramic (CGC) powder (1wt%) or CGC powder extracts ($[Cu]_{Tot}$ = ~200ppm) with various extract additives (triethyl phosphite (TEP) or diphenyl phosphate (DPP) with and without a base, 2-Amino-2-methyl-1-propanol (AMP-95). **A.** Average log-kill values against *S. aureus*. Control sample has no antimicrobial additive (CGC powder or CGC powder extract). The bar labeled "H_2O" represents a CGC powder extraction with water only (no additives). Error bars represent the standard deviation of duplicate samples. **B.** Measured paint film color differences. **C.** Visual representation of the measured color swatches.

View Article Online
DOI: 10.1039/D4LF00235K

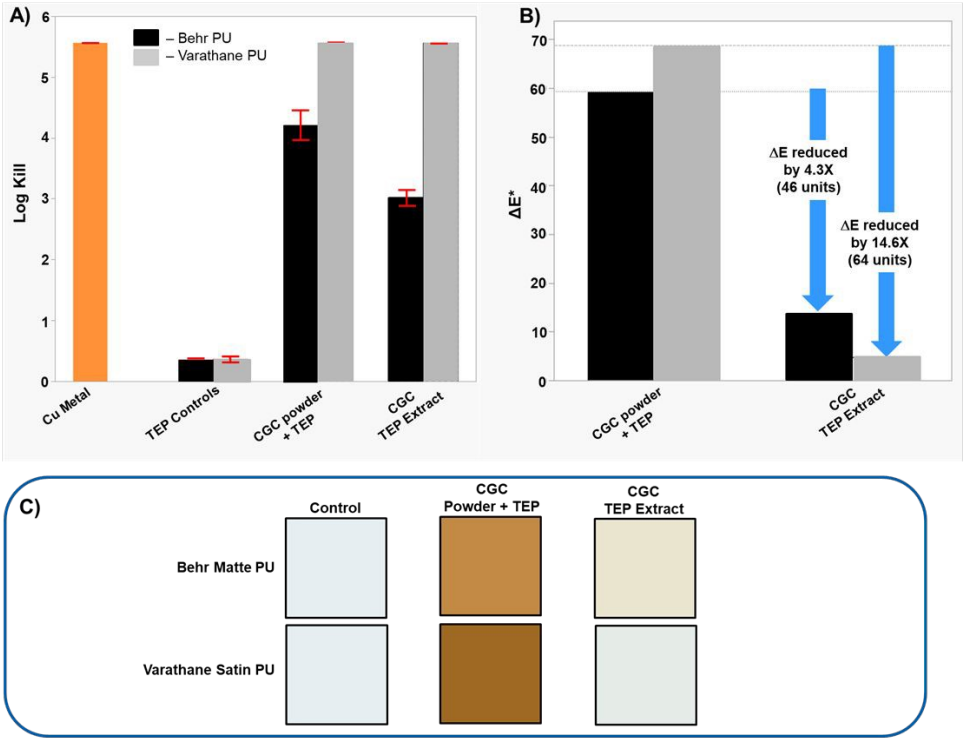

Figure 6. Antimicrobial efficacy and color results for two water-based polyurethane (PU) wood coating dry films dosed with copper glass-ceramic (CGC) powder (5wt%) or CGC powder extracts with triethyl phosphite (TEP) ($[Cu]_{Tot}$ = 1,000ppm). **A.** Average log-kill values against *S. aureus* for paint films dosed with CGC powder or CGC powder extracts. TEP controls are coatings with TEP only (no CGC powder nor CGC powder extract). Error bars represent the standard deviation of duplicate samples. **B.** Measured wood coating film color differences. **C.** Visual representation of the measured color swatches.

View Article Online
DOI: 10.1039/D4LF00235K

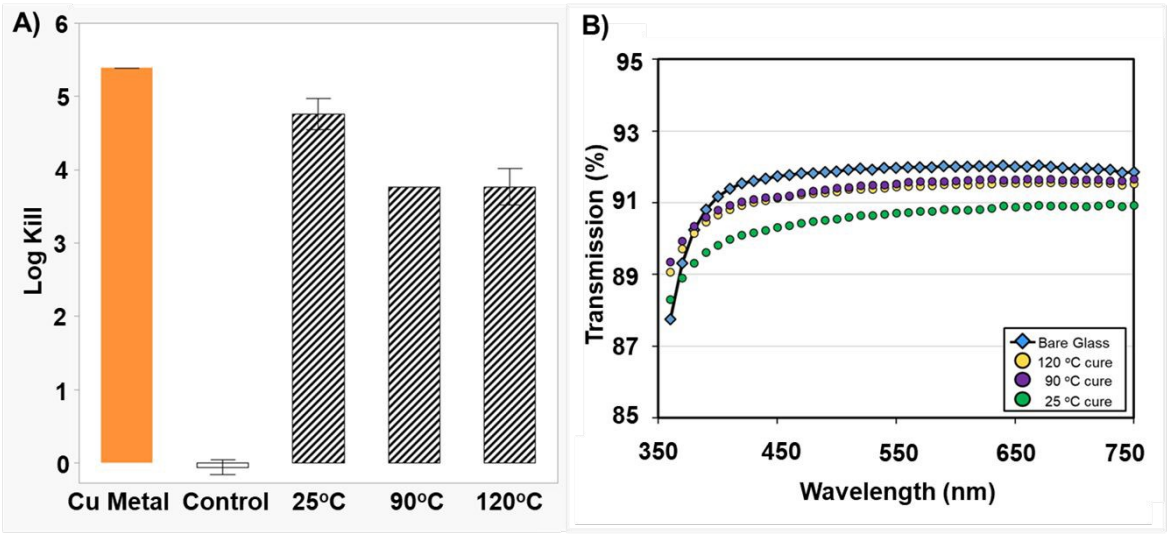

Figure 7. Antimicrobial efficacy and optical transmission results for Ferro 221 glass coatings dosed with copper glass-ceramic (CGC) powder extracts with triethyl phosphite (TEP) ($[Cu]_{Tot}$ = 600ppm) and cured at different temperatures. **A.** Average log-kill values against *S. aureus* for various coating cure conditions. Control sample has no antimicrobial additive. Error bars represent the standard deviation of duplicate samples. **B.** Optical transmission measurements.

View Article Online
DOI: 10.1039/D4LF00235K

The data supporting this article have been included as part of the Supplementary Information.